

Coupled channel Faddeev calculations of a $\bar{K}N\pi$ quasibound state

A. Gal^{1,*} and H. Garcilazo^{2,†}

¹*Racah Institute of Physics, The Hebrew University, Jerusalem 91904, Israel*

²*Escuela Superior de Física y Matemáticas*

Instituto Politécnico Nacional, Edificio 9, 07738 México D.F., Mexico

(Dated: September 24, 2018)

Abstract

The $\bar{K}N\pi$ system is studied using separable interactions fitted to data available on the s -wave $\bar{K}N\pi$ subsystem and the p -wave πN , πY , $\pi\pi$ and $\pi\bar{K}$ subsystems. Three-body $\bar{K}N\pi\pi$ coupled channel Faddeev equations with relativistic kinematics are solved in search for poles in the complex energy plane. A $\bar{K}N\pi$ quasibound pole with quantum numbers $I(J^P) = 1(\frac{3}{2}^-)$ is found near and below the $\bar{K}N\pi$ threshold, its precise location depending sensitively on the poorly known shape of the p -wave πY interaction. This $\bar{K}N\pi$ quasibound state suggests the existence of a D_{13} Σ resonance with width about 60 MeV near threshold ($M \approx 1570$ MeV), excluding meson absorption contributions.

PACS numbers: 13.75.Gx, 13.75.Jz, 13.75.Lb, 11.80.Jy

Keywords: pion-baryon interactions, kaon-baryon interactions, meson-meson interactions, Faddeev equations

*Electronic address: avragal@vms.huji.ac.il

†Electronic address: humberto@esfm.ipn.mx

I. INTRODUCTION

Meson assisted dibaryons are three-body systems consisting of two unbound baryons plus a p -wave pion [1]. For strangeness $\mathcal{S} = -1$, a prototype $I(J^P) = \frac{3}{2}(2^+)$ $YN\pi$ quasibound state ($Y \equiv$ hyperon), driven by the p -wave resonances $\Delta(1232)$ and $\Sigma(1385)$, was studied recently [2, 3]. Replacing a baryon in this system by a meson, one obtains a two-meson assisted baryon. For example, staying within $\mathcal{S} = -1$ and substituting \bar{K} meson for hyperon Y , or π meson for nucleon N , a coupled channel $\bar{K}N\pi$ – $Y\pi\pi$ two-meson assisted baryon resonance is obtained. In the present paper we study this three body system by solving coupled channel, kinematically relativistic Faddeev equations. Considering the three-body $\bar{K}N\pi$ channel, its $\bar{K}N$ subsystem is dominated by the $I(J^P) = 0(\frac{1}{2}^-)$ channel in which the $\bar{K}N - \pi\Sigma$ coupled channel s -wave interaction is already sufficiently strong to bind, resulting in the s -wave $\Lambda(1405)$ resonance. The πN subsystem is dominated by the $I(J^P) = \frac{3}{2}(\frac{3}{2}^+)$ channel, resulting in the p -wave $\Delta(1232)$ resonance, and the $\pi\bar{K}$ subsystem is dominated by the $I(J^P) = \frac{1}{2}(1^-)$ channel, resulting in the $\bar{K}^*(892)$ resonance. In addition, since the $\bar{K}N - \pi Y$ coupling connects $\bar{K}N\pi$ to $\pi Y\pi$, one must also consider the πY subsystem in the $I(J^P) = 1(\frac{3}{2}^+)$ channel, resulting in the p -wave $\Sigma(1385)$ resonance, and the $\pi\pi$ subsystem in the $I(J^P) = 1(1^-)$ channel, resulting in the p -wave $\rho(770)$ resonance. It is straightforward to see that the only three-body configuration in which these subsystem quantum number specifications can be accommodated is $I(J^P) = 1(\frac{3}{2}^-)$. The value of spin $J^P = \frac{3}{2}^-$ is maximal for a p -wave pion and s -wave nucleon and \bar{K} meson, thus ensuring that each one of the two-body channels has precisely the spin at which it resonates. The value of isospin $I = 1$ is not maximal, which means that nonresonating two-body channels will also contribute to the binding energy balance of $I(J^P) = 1(\frac{3}{2}^-)$ $\bar{K}N\pi$. The corresponding interactions are disregarded with respect to those in the resonating channels in this exploratory calculation. Other allowed values of isospin, $I = 0, 2$, stand no chance of producing three-body binding because only one of the three possible two-body resonating channels can contribute to the $I = 0, 2$ $\bar{K}N\pi$ states. Thus, the choice $I(J^P) = 1(\frac{3}{2}^-)$ is unique in searching for quasibound configurations of $\bar{K}N\pi$. It is worth noting that the $\bar{K}N\pi$ threshold around 1570 MeV is within a close reach of the one-star $I(J^P) = 1(\frac{3}{2}^-)$ $\Sigma(1580)$ ‘exotic’ resonance [4]. This apparent connection is discussed towards the conclusion of the present paper.

Other studies of two-meson assisted baryonic resonances focused entirely on s -wave two-

body interactions, for nonstrange resonances [5–8] as well as for strangeness $\mathcal{S} = -1$ [9] and $\mathcal{S} = -2$ [10]. For $\mathcal{S} = -1$, in particular, the $I(J^P) = 0, 1(\frac{1}{2}^+)$ $\bar{K}N\pi$ configurations were studied, with Λ and Σ resonance candidates in the mass range $M \sim 1.6 - 1.8$ GeV. It is remarkable that with meson-baryon p -wave interactions, as studied here, a lower mass value can be reached which, furthermore, corresponds to a quasibound state rather than resonance. Finally, we mention the $KN\pi$ Faddeev calculation in Ref. [11], again with s -wave two-body interactions, searching for a $\frac{1}{2}^+$ exotic $\mathcal{S} = +1$ Θ^+ pentaquark. We have verified by solving the appropriate Faddeev equations with a p -wave pion that no $\frac{3}{2}^-$ $KN\pi$ quasibound state candidate exists in the relevant energy range for a $\mathcal{S} = +1$ Θ^+ pentaquark.

The paper is organized as follows. In Sec. II we construct two-body separable interactions for the resonating channels discussed above. The corresponding t matrices serve as input to the set of three-body coupled Faddeev equations which are constructed in Sec. III. We employ a straightforward generalization of the nonrelativistic Faddeev equations, incorporating relativistic kinematics to account in a minimal way for the light pion in the $\bar{K}N\pi\text{--}\pi Y\pi$ coupled three-body systems. Solving these Faddeev equations we find a $\bar{K}N\pi$ quasibound pole which is listed for several allowed parametrizations of the πY two-body data and is discussed in Sec. IV. Our calculations, suggesting a D_{13} Σ resonance near the $\bar{K}N\pi$ threshold ($M \approx 1570$ MeV), are summarized in the last Sec. V.

II. SEPARABLE TWO-BODY INTERACTIONS INPUT

Data available on the $\bar{K}N\text{--}\pi Y$, πN , $\pi\bar{K}$, and $\pi\pi$ subsystems were fitted with rank-one energy independent separable potentials, as detailed below. While the p -wave subsystems in the mass range considered in this work are dominated each by a single resonance pole with no other nearby threshold to introduce additional significant energy dependence, this may not hold for the s -wave $\bar{K}N\text{--}\pi Y$ subsystem where energy dependence affects the number and position of poles (see Ref. [12] for a recent review). However, energy dependent potentials are known to cause problems in relativistically formulated three-body calculations [13]. We further remark on energy dependence in subsection III A. For a standard classification of the two-body subsystems, we denote \bar{K} as particle 1, N as particle 2, π as particle 3, and label the two-body t -matrices by the spectator particle. Thus, t_1 is the πN t -matrix, t_2 is the $\bar{K}\pi$ t -matrix, and t_3 is the $\bar{K}N$ t -matrix. In addition, we introduce t_4 as the $\pi\pi$ t -matrix.

A. The $\bar{K}N - \pi\Sigma - \pi\Lambda$ subsystem

The $\bar{K}N$ interaction allows particle conversion to $\pi\Sigma$ and $\pi\Lambda$. There are two resonating two-body channels that contribute to the $I(J^P) = 1(\frac{3}{2}^-)$ three-body state. One is the $I(J^P) = 0(\frac{1}{2}^-)$ channel which results in the s -wave $\Lambda(1405)$ resonance and the other one is the $I(J^P) = 1(\frac{3}{2}^+)$ channel, resulting in the p -wave $\Sigma(1385)$ resonance. We use the Lippmann-Schwinger equation with relativistic kinematics

$$t_3^{\alpha\beta}(p, p''; w_0) = V_3^{\alpha\beta}(p, p'') + \sum_{\gamma=\bar{K}N, \pi\Sigma, \pi\Lambda} \int_0^\infty p'^2 dp' V_3^{\alpha\gamma}(p, p') \frac{1}{w_0 - w_\gamma(p') + i\epsilon} \times t_3^{\gamma\beta}(p', p''; w_0); \quad \alpha, \beta = \bar{K}N, \pi\Sigma, \pi\Lambda, \quad (1)$$

where w_0 is the invariant mass of the two-body subsystem and

$$w_{ab}(p) = \sqrt{m_a^2 + p^2} + \sqrt{m_b^2 + p^2}. \quad (2)$$

Using the separable interaction

$$V_3^{\alpha\beta}(p, p') = g_\alpha(p) \lambda_3 g_\beta(p'), \quad (3)$$

the solution of Eq. (1) is

$$t_3^{\alpha\beta}(p, p'; w_0) = g_\alpha(p) \tau_3(w_0) g_\beta(p'), \quad (4)$$

with

$$\tau_3^{-1}(w_0) = \frac{1}{\lambda_3} - \sum_{\alpha=\bar{K}N, \pi\Sigma, \pi\Lambda} \int_0^\infty p^2 dp \frac{g_\alpha^2(p)}{w_0 - w_\alpha(p) + i\epsilon}. \quad (5)$$

1. s waves

In the case of the isospin $I_3 = 0$ $\Lambda(1405)$ s -wave resonance, the $I_{\pi\Lambda} = 1$ $\pi\Lambda$ channel is excluded by isospin conservation, so that only the channels $\bar{K}N$ and $\pi\Sigma$ contribute. The corresponding form factors were parametrized by Yamaguchi forms:

$$g_{\bar{K}N}^s(p) = \frac{1}{c_{\bar{K}N}^2 + p^2}, \quad g_{\pi\Sigma}^s(p) = \frac{1}{c_{\pi\Sigma}^2 + p^2}, \quad (6)$$

with $g_{\pi\Lambda}^s(p) = 0$. It is worth pointing out that a single-channel energy independent separable potential of the form (3) does not generate s -wave resonances, which becomes possible upon

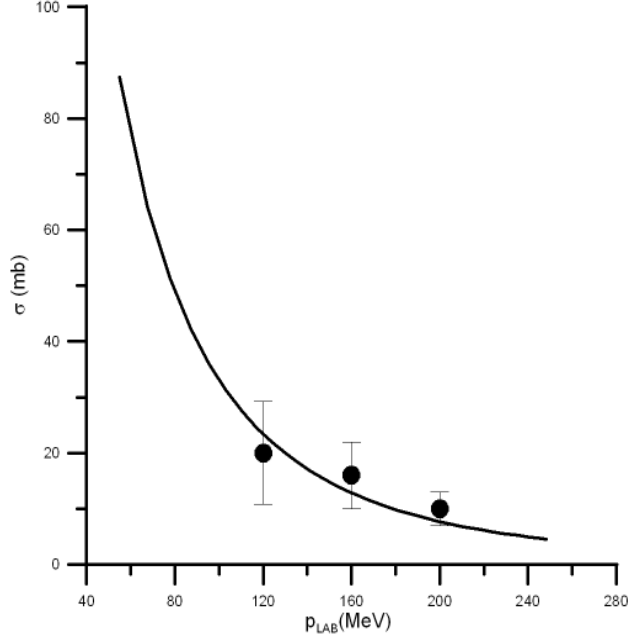


FIG. 1: Low energy $K^-p \rightarrow \pi^0 \Sigma^0$ cross sections [14]. The solid curve results from the $I_3 = 0$ separable interaction (6) with parameters listed in Table I.

including a second channel. Note that even with three channels, Eq. (3) is a rank-one separable potential since it has only one strength parameter λ_3 . The three parameters of our $I_3 = 0$ $\bar{K}N$ - $\pi\Sigma$ separable interaction model, λ_3^s , $c_{\bar{K}N}$, and $c_{\pi\Sigma}$ are listed in Table I. They were adjusted to reproduce the PDG position and width of the $\Lambda(1405)$ resonance [4] as well as the low-energy cross sections shown in Fig. 1 for the pure $I_3 = 0$ $K^-p \rightarrow \pi^0 \Sigma^0$ reaction. We did not use the more comprehensive data from $K^-p \rightarrow \pi^\pm \Sigma^\mp$ because these reactions require information on the $I_3 = 1$ $\bar{K}N$ - $\pi\Sigma$ - $\pi\Lambda$ s -wave subsystem which is nonresonant and is excluded from the present calculation. Preliminary test calculations including the $I_3 = 1$ s -wave channel produced negligible effects.

TABLE I: Parameters of the $I_3 = 0$ $\bar{K}N - \pi\Sigma$ separable s -wave interaction.

$\lambda_3^s(\text{fm}^{-2})$	$c_{\bar{K}N}(\text{fm}^{-1})$	$c_{\pi\Sigma}(\text{fm}^{-1})$
-3.3391	2.0	2.5346

2. p waves

In the case of the $I_3 = 1$ $\Sigma(1385)$ p -wave resonance, the three channels $\bar{K}N$, $\pi\Sigma$, and $\pi\Lambda$ are all allowed; however, there is some evidence that the $\bar{K}N$ channel couples very weakly to the $\Sigma(1385)$ resonance [15, 16] so that one may consider only the $\pi\Lambda$ and $\pi\Sigma$ channels. Since in this case the form factors $g_\alpha(p)$ must be of a p -wave type, we took them in the form

$$g_{\pi\Lambda}^p(p) = p(1 + Ap^2)e^{-p^2/\gamma^2}, \quad g_{\pi\Sigma}^p(p) = Bg_{\pi\Lambda}^p(p), \quad (7)$$

with $g_{\bar{K}N}^p(p) = 0$. In this case we know only the position, width, and branching ratio for decay of the $\Sigma(1385)$ resonance into the $\pi\Lambda$ and $\pi\Sigma$ channels. Thus, we have three pieces of data to fit our interaction model which contains four parameters (λ_3^p , γ , A , B) so that we can take one of these as a free parameter and fit the other three. We show in Table II the parameters λ_3^p , γ and B , upon gridding on A between 0 to 0.5. These parameters differ from those used in the nonrelativistic calculation of Ref. [3].

TABLE II: Parameters of the $\pi\Sigma - \pi\Lambda$ separable interaction (7) in the $I_3 = 1$ channel for several values of the parameter A . Values of the r.m.s. momentum $\langle p^2 \rangle_g^{\frac{1}{2}}$ (in fm^{-1}) of the form factor $g_{\pi Y}^p(p)$, the r.m.s. distance $\langle r^2 \rangle_{\tilde{g}}^{\frac{1}{2}}$ and the zero r_0 (both in fm) of the Fourier transform $\tilde{g}_{\pi Y}^p(r)$ are also listed.

$A(\text{fm}^2)$	$\lambda_3^p(\text{fm}^4)$	$\gamma(\text{fm}^{-1})$	B	$\langle p^2 \rangle_g^{\frac{1}{2}}$	$\langle r^2 \rangle_{\tilde{g}}^{\frac{1}{2}}$	r_0
0.00	-0.0077258	4.9091	0.87039	6.94	0.58	—
0.05	-0.0083840	3.6156	0.87871	5.79	0.56	1.11
0.10	-0.0088725	3.1595	0.89220	5.16	0.52	1.19
0.15	-0.0091172	2.8951	0.90689	4.77	0.47	1.25
0.20	-0.0092049	2.7147	0.92184	4.50	0.41	1.31
0.25	-0.0091851	2.5810	0.93671	4.30	0.33	1.36
0.30	-0.0090934	2.4765	0.95132	4.13	0.23	1.41
0.35	-0.0089513	2.3919	0.96559	4.00	—	1.45
0.40	-0.0087763	2.3216	0.97949	3.89	—	1.48
0.45	-0.0085787	2.2619	0.99298	3.80	—	1.51
0.50	-0.0083686	2.2105	1.00606	3.72	—	1.54

Listed also in the table are $\langle p^2 \rangle^{\frac{1}{2}}$ values for $g_{\pi Y}^p(p)$, plus $\langle r^2 \rangle^{\frac{1}{2}}$ and zeros r_0 for its Fourier transform $\tilde{g}_{\pi Y}^p(r)$. These form-factor sizes will be discussed and compared in subsection II E with those for the p -wave form factors derived below for other subsystems.

B. The πN subsystem

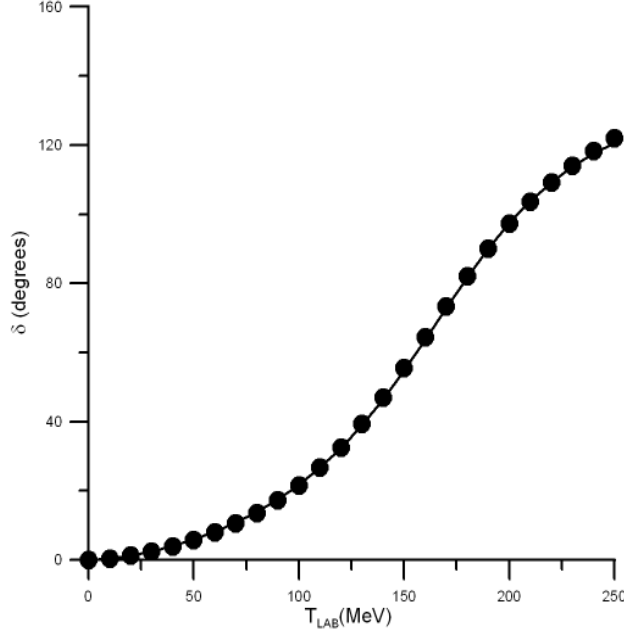


FIG. 2: The πN P_{33} phase shift across the $\Delta(1232)$ resonance. The solid curve is obtained by using the πN form factor parameters, Eq. (11), listed in Table III. The circles are from Ref. [17] with errors (suppressed in the figure) that are less than the thickness of the line.

The πN p -wave interaction is dominated by the P_{33} channel through the $\Delta(1232)$ resonance and we use for it, as well as for the remaining two-body subsystems, a rank-one separable potential

$$V_1(p, p') = g_1(p) \lambda_1 g_1(p'), \quad (8)$$

the t -matrix of which is

$$t_1(p, p'; w_0) = g_1(p) \tau_1(w_0) g_1(p'), \quad (9)$$

with

$$\tau_1^{-1}(w_0) = \frac{1}{\lambda_1} - \int_0^\infty p^2 dp \frac{g_1^2(p)}{w_0 - w_{\pi N}(p) + i\epsilon}. \quad (10)$$

The πN form factor, as well as for the subsequent two-body subsystems, is chosen as

$$g_1(p) = p[e^{-p^2/\beta^2} + Cp^2e^{-p^2/\alpha^2}]. \quad (11)$$

We show in Fig. 2 the fit to the P_{33} phase shift of Ref. [17] obtained with the set of πN parameters given in the first line of Table III.

C. The $\pi\bar{K}$ subsystem

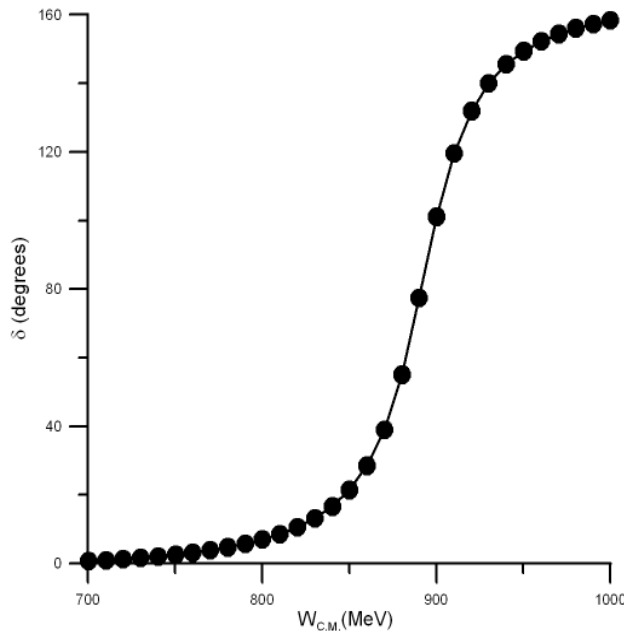


FIG. 3: The $I_2 = \frac{1}{2}$, $J_2 = 1$ p -wave $\pi\bar{K}$ phase shift across the $\bar{K}^*(892)$ resonance. The solid curve is obtained by using the $\pi\bar{K}$ form factor parameters, Eq. (11), listed in Table III. The circles are from Ref. [18] with errors (suppressed in the figure) that are less than the thickness of the line.

The separable interaction $V_2(p, p') = g_2(p)\lambda_2g_2(p')$ corresponding to the $\pi\bar{K}$ subsystem is chosen such that the $\pi\bar{K}$ form factor $g_2(p)$ is functionally identical with $g_1(p)$, Eq. (11), for πN . To fix the parameters of $g_2(p)$, we used the phase shift by Boito *et al.* fitted to $\tau \rightarrow K\pi\nu_\tau$ and K_{ℓ_3} decays [18]. These parameters are listed in the second line of Table III, and the agreement with this phase shift is shown in Fig. 3.

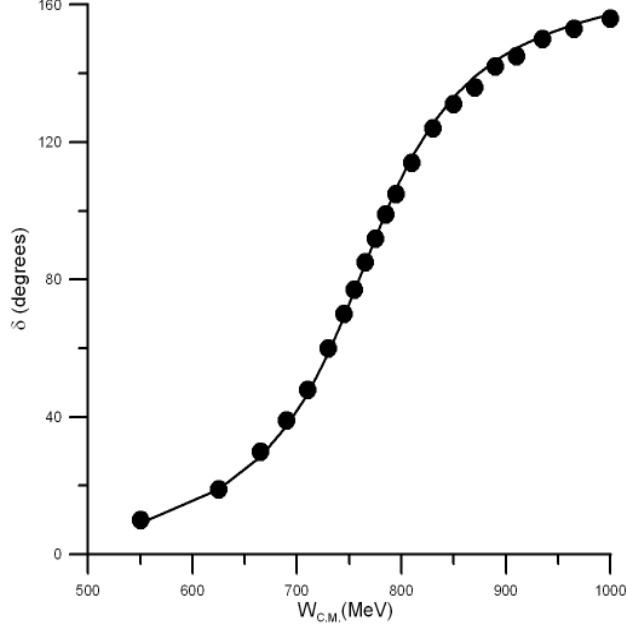


FIG. 4: The $I_4 = 1, J_4 = 1$ p -wave $\pi\pi$ phase shift across the $\rho(770)$ resonance. The solid curve is obtained by using the $\pi\pi$ form factor parameters, Eq. (11), listed in Table III. The circles are from Ref. [19] with slight errors suppressed in the figure.

D. The $\pi\pi$ subsystem

Since this subsystem is reached only following $\bar{K}N \rightarrow \pi Y$ conversion, we denote its t matrix by t_4 . The separable interaction $V_4(p, p') = g_4(p)\lambda_4 g_4(p')$ is given again by a form factor $g_4(p)$ which is functionally identical with $g_1(p)$, Eq. (11), for πN . We fitted the $\pi\pi$ $I = J = 1$ p -wave phase shift obtained in Ref. [19], as shown in Fig. 4, using the set of parameters given in the last line of Table III.

TABLE III: Parameters of the πN , $\pi\bar{K}$, and $\pi\pi$ separable p -wave interactions, with form factors $g(p)$ given by Eq. (11). Values of the r.m.s. momentum $\langle p^2 \rangle_g^{\frac{1}{2}}$ (in fm^{-1}), the r.m.s. distance $\langle r^2 \rangle_{\tilde{g}}^{\frac{1}{2}}$ of the Fourier transform $\tilde{g}(r)$ and its zero r_0 (both in fm) are also listed.

subsystem	$\lambda(\text{fm}^4)$	$\alpha(\text{fm}^{-1})$	$\beta(\text{fm}^{-1})$	$C(\text{fm}^2)$	$\langle p^2 \rangle^{\frac{1}{2}}$	$\langle r^2 \rangle^{\frac{1}{2}}$	r_0
πN	-0.075869	2.3668	1.04	0.23	4.07	1.47	1.36
$\pi\bar{K}$	-0.0037111	4.3057	1.703	0.122	7.46	0.93	0.74
$\pi\pi$	-0.0078958	5.6646	1.89	0.03	9.81	0.88	0.56

E. Form factor sizes

The form factors $g(p)$, Eq. (11), with parameters fitted to phase shift analyses of the corresponding p -wave resonances as listed in Table III, all have r.m.s. values $\langle p^2 \rangle^{\frac{1}{2}}$ larger than 4 fm^{-1} , suggesting naively spatial extensions of less than 0.25 fm . If this were true, the usefulness of treating the $\bar{K}N\pi$ system in terms of hadronic degrees of freedom would have become questionable. However, the uncertainty principle places only a lower bound on the spatial extension and indeed the $\langle r^2 \rangle^{\frac{1}{2}}$ values listed in the table are considerably larger than 0.25 fm , thus qualifying for hadronic attributes. These r.m.s. radii were calculated for $\tilde{g}(r)$, where $\tilde{g}(\vec{r}) = \hat{r}\tilde{g}(r)$ is the Fourier transform of the p -wave form factor $g(\vec{p}) = \hat{p}g(p)$. Up to a constant,

$$\tilde{g}(r) = \int j_1(pr)g(p)p^2 dp, \quad (12)$$

with j_1 the spherical Bessel function for $\ell = 1$. Unlike $g(p)$, $\tilde{g}(r)$ is not positive definite, it flips from positive below r_0 to negative above r_0 . This may result in negative values of $\langle r^2 \rangle$, as observed in Table II for some of the πY form factors, and in grossly underestimated sizes for those form factors for which $\langle r^2 \rangle$ is still positive. For this reason, we prefer to use r_0 as an alternative spatial size parameter. The values assumed by r_0 in Table III, although smaller than the corresponding $\langle r^2 \rangle^{\frac{1}{2}}$ values, still qualify for being considered as hadronic sizes. It is reassuring that the values of r_0 for πY in Table II are all larger than 1 fm . A crude way to relate the expected range of values of r_0 for πY to the value of r_0 for πN is to note that the energy excitation from Λ to $\Sigma(1385)$ is somewhat less than from N to $\Delta(1232)$, and therefore r_0 for πY should be a bit larger than r_0 for πN , judging also by the systematics of $\pi\bar{K}$ with respect to $\pi\pi$ in Table III. We therefore estimate that r_0 for πY is roughly up to 0.15 fm larger than for πN , i.e., in the range $1.36\text{--}1.51 \text{ fm}$. This argument suggests that among the πY form factors listed in Table II, only those in the range $A = 0.25$ to $A = 0.45 \text{ fm}^2$ are consistent with the form-factor phenomenology used for the other subsystems.

III. THREE-BODY EQUATIONS

A. Two-body t -matrix in a three-body system

To embed the two-body subsystems discussed in Sec. II into the three-body system, Eq. (10) needs to be generalized to

$$\tau_1^{-1}(W_0; q) = \frac{1}{\lambda_1} - \int_0^\infty p^2 dp \frac{g_1^2(p)}{W_0 - \sqrt{q^2 + m_{\bar{K}}^2} - \sqrt{q^2 + w_{\pi N}^2(p)} + i\epsilon}, \quad (13)$$

where W_0 is the invariant mass of the three-body system and $m_{\bar{K}}$ and q are the mass and momentum of the spectator particle in the three-body c.m. frame. Similar expressions apply to the other subsystems. In the case of the amplitude t_4 the mass of the spectator particle can be either m_Σ or m_Λ so that this amplitude is of the form $\tau_4^Y(W_0; q)$. We note that in the three-body c.m. frame, in which the Faddeev equations are formulated and solved, the two-body ‘in medium’ isobar propagators input $\tau(W_0; q)$ are energy dependent even though the underlying two-body separable potentials are energy independent. The τ ’s depend also on the spectator momentum q , reducing to the two-body momentum independent t ’s of Eq. (10) for $q = 0$.

B. Three-body Faddeev equations

Allowing for particle conversion, there are two possible three-body states $\bar{K}N\pi$ and $\pi Y\pi$ which we will refer as a and b , respectively. Therefore, the Green’s function for three free particles is a 2×2 matrix of the form

$$G_0 = \begin{pmatrix} G_a & 0 \\ 0 & G_b \end{pmatrix} = \begin{pmatrix} G_a & 0 \\ 0 & 0 \end{pmatrix} + \begin{pmatrix} 0 & 0 \\ 0 & G_b \end{pmatrix} \equiv G_0^a + G_0^b, \quad (14)$$

with

$$G_a = \frac{1}{W_0 - \sqrt{m_{\bar{K}}^2 + q_1^2} - \sqrt{m_N^2 + q_2^2} - \sqrt{m_\pi^2 + q_3^2} + i\epsilon}, \quad (15)$$

$$G_b = \frac{1}{W_0 - \sqrt{m_\pi^2 + q_1^2} - \sqrt{m_Y^2 + q_2^2} - \sqrt{m_\pi^2 + q_3^2} + i\epsilon}. \quad (16)$$

Since particle conversion is effected only through the amplitude t_3 , the three-body Faddeev equations take the form

$$T_1 = t_1 G_0^a T_2 + t_1 G_0^a T_3, \quad (17)$$

$$T_2 = t_2 G_0^a T_1 + t_2 G_0^a T_3, \quad (18)$$

$$T_3 = t_3 G_0^a T_1 + t_3 G_0^a T_2 + t_3 G_0^b T_3 + 2t_3 G_0^b T_4, \quad (19)$$

$$T_4 = t_4 G_0^b T_3. \quad (20)$$

Here, T_i is that part of the three-body amplitude where in the last stage particle i is spectator while particles j and k interact. Particle conversion is generated exclusively through the two-body amplitude t_3 in the last two terms on the r.h.s. of Eq. (19). T_4 represents that part of the three-body amplitude where in the last stage the hyperon is spectator while the two pions interact, so that T_4 couples to T_3 in Eq. (19) through pion exchange and the factor 2 arises because any one of the two pions may be exchanged. The amplitude T_3 can couple to itself as a consequence of hyperon exchange.

The two-body t -matrices constructed in the previous section can be written in the space $\begin{pmatrix} a \\ b \end{pmatrix}$ as 2×2 matrices of the form

$$t_i = |g_i\rangle \begin{pmatrix} \tau_i & 0 \\ 0 & 0 \end{pmatrix} \langle g_i|; \quad i = 1, 2, \quad (21)$$

$$t_3 = \begin{pmatrix} |g_{\bar{K}N}\rangle \\ |g_{\pi Y}\rangle \end{pmatrix} \tau_3 \left(\langle g_{\bar{K}N}| \quad \langle g_{\pi Y}| \right), \quad (22)$$

$$t_4 = |g_4\rangle \begin{pmatrix} 0 & 0 \\ 0 & \tau_4 \end{pmatrix} \langle g_4|, \quad (23)$$

so that the Faddeev components are of the form

$$T_i = |g_i\rangle \begin{pmatrix} X_i \\ 0 \end{pmatrix}; \quad i = 1, 2, \quad (24)$$

$$T_3 = \begin{pmatrix} |g_{\bar{K}N}\rangle \\ |g_{\pi Y}\rangle \end{pmatrix} X_3, \quad (25)$$

$$T_4 = |g_4\rangle \begin{pmatrix} 0 \\ X_4 \end{pmatrix}. \quad (26)$$

Substituting Eqs. (21)-(26) into the Faddeev equations (17)-(20), we get the equations for the amplitudes X_i

$$X_i = \tau_i \langle g_i | G_a | g_{3-i} \rangle X_{3-i} + \tau_i \langle g_i | G_a | g_{\bar{K}N} \rangle X_3, \quad i = 1, 2 \quad (27)$$

$$X_3 = \tau_3 \sum_{j=1}^2 \langle g_{\bar{K}N} | G_a | g_j \rangle X_j + \tau_3 \langle g_{\pi Y} | G_b | g_{\pi Y} \rangle X_3 + 2\tau_3 \langle g_{\pi Y} | G_b | g_4 \rangle X_4, \quad (28)$$

$$X_4 = \tau_4 \langle g_4 | G_b | g_{\pi Y} \rangle X_3. \quad (29)$$

These equations take the explicit form

$$X_i(q_i) = \tau_i(W_0; q_i) \int_0^\infty dq_{3-i} K_{i(3-i)}(q_i, q_{3-i}) X_{3-i}(q_{3-i}) + \tau_i(W_0; q_i) \sum_{I_3=0,1} \int_0^\infty dq_3 K_{i3}^{I_3}(q_i, q_3) X_3^{I_3}(q_3), \quad i = 1, 2, \quad (30)$$

$$X_3^{I_3}(q_3) = \tau_3^{I_3}(W_0; q_3) \sum_{j=1}^2 \int_0^\infty dq_j K_{3j}^{I_3}(q_i, q_j) X_j(q_j) + \tau_3^{I_3}(W_0; q_3) \sum_{I'_3=0,1} \int_0^\infty dq_1 K_{33}^{I_3 I'_3}(q_3, q_1) \times X_3^{I'_3}(q_1) + 2\tau_3^{I_3}(W_0; q_3) \sum_{Y=\Sigma, \Lambda} \int_0^\infty dq_2 K_{34}^{I_3 Y}(q_3, q_2) X_4^Y(q_2), \quad I_3 = 0, 1, \quad (31)$$

$$X_4^Y(q_2) = \tau_4^Y(W_0; q_2) \sum_{I_3=0,1} \int_0^\infty dq_3 K_{43}^{Y I_3}(q_2, q_3) X_3^{I_3}(q_3); \quad Y = \Sigma, \Lambda, \quad (32)$$

where the dependence of the amplitudes X_i and the kernels K_{ij} on the total energy W_0 was suppressed. The amplitudes X_i depend each on its spectator momentum q_i . These spectator momenta are related by the three-body c.m. constraint which is evident upon inspecting the expressions for the kernels K_{ij} :

$$K_{12}(q_1, q_2) = \frac{q_1 q_2}{2} \int_{-1}^1 d\cos\theta \frac{g_1(p_1)(\hat{p}_1 \cdot \hat{p}_2) g_2(p_2) b_{12}^{\frac{3}{2}\frac{1}{2}}}{W_0 - \sqrt{m_K^2 + q_1^2} - \sqrt{m_N^2 + q_2^2} - \sqrt{m_\pi^2 + (\vec{q}_1 + \vec{q}_2)^2} + i\epsilon}, \quad (33)$$

$$K_{31}^{I_3}(q_3, q_1) = \frac{q_3 q_1}{2} \int_{-1}^1 d\cos\theta \frac{g_{\bar{K}N}^{I_3}(p_3)(\hat{\kappa}_3 \cdot \hat{p}_1) g_1(p_1) b_{31}^{I_3 \frac{3}{2}}}{W_0 - \sqrt{m_\pi^2 + q_3^2} - \sqrt{m_K^2 + q_1^2} - \sqrt{m_N^2 + (\vec{q}_3 + \vec{q}_1)^2} + i\epsilon}, \quad (34)$$

$$K_{23}^{I_3}(q_2, q_3) = \frac{q_2 q_3}{2} \int_{-1}^1 d\cos\theta \frac{g_2(p_2)(\hat{p}_2 \cdot \hat{\kappa}_3) g_{\bar{K}N}^{I_3}(p_3) b_{23}^{\frac{1}{2} I_3}}{W_0 - \sqrt{m_N^2 + q_2^2} - \sqrt{m_\pi^2 + q_3^2} - \sqrt{m_K^2 + (\vec{q}_2 + \vec{q}_3)^2} + i\epsilon}, \quad (35)$$

$$K_{33}^{I_3 I'_3}(q_3, q_1) = \frac{q_3 q_1}{2} \sum_{Y=\Sigma, \Lambda} \int_{-1}^1 d\cos\theta \frac{g_{\pi Y}^{I_3}(p_3)(\hat{\kappa}_3 \cdot \hat{\kappa}_1) g_{\pi Y}^{I'_3}(p_1) b_{31}^{I_3 I'_3}}{W_0 - \sqrt{m_\pi^2 + q_3^2} - \sqrt{m_\pi^2 + q_1^2} - \sqrt{m_Y^2 + (\vec{q}_3 + \vec{q}_1)^2} + i\epsilon}, \quad (36)$$

$$K_{43}^{YI_3}(q_2, q_3) = \frac{q_2 q_3}{2} \int_{-1}^1 d\cos\theta \frac{g_4(p_2)(\hat{p}_2 \cdot \hat{\kappa}_3)g_{\pi Y}^{I_3}(p_3)b_{23}^{1I_3}}{W_0 - \sqrt{m_\pi^2 + q_2^2} - \sqrt{m_\pi^2 + q_3^2} - \sqrt{m_Y^2 + (\vec{q}_2 + \vec{q}_3)^2} + i\epsilon}, \quad (37)$$

where the dependence on the total energy W_0 in the arguments of the kernels K_{ij} was again suppressed. In Eqs. (34)-(37) $\hat{\kappa}_i = \hat{q}_i$ if $I_3 = 0$ and $\hat{\kappa}_i = \hat{p}_i$ if $I_3 = 1$.

The isospin recoupling coefficients are

$$b_{ij}^{I_i I_j} = (-)^{I_j + \tau_j - I} \sqrt{(2I_i + 1)(2I_j + 1)W(\tau_j \tau_k I \tau_i; I_i I_j)}, \quad (38)$$

with W the Racah coefficient. $I = 1$ is the total isospin and τ_1, τ_2, τ_3 are the isospins of the three particles. In the first three kernels the three particles are \bar{K}, N, π and in the last two kernels they are π, Y, π .

From Eqs. (33)-(37) one obtains the other necessary expressions by using $K_{ji}(q_j, q_i) = K_{ij}(q_i, q_j)$, etc. As for p_i , the magnitude of the relative three-momentum \vec{p}_i , it is Lorentz invariant since it is expressible in terms of the invariant mass of the relative momentum four-vector, see Eqs. (28)–(30) in Ref. [2]. The details of the relativistic boost involved in expressing \vec{p}_i in the three-body c.m. system were recorded in Eqs. (32)–(33) there and are adapted below to the present notations. Thus, one can calculate $p_i, p_j, (\hat{p}_i \cdot \hat{p}_j), (\hat{q}_i \cdot \hat{p}_j)$, and $(\hat{p}_i \cdot \hat{q}_j)$ by using

$$\vec{p}_i = -\vec{q}_j - a_{ij}\vec{q}_i, \quad \vec{p}_j = \vec{q}_i + a_{ji}\vec{q}_j, \quad (39)$$

where i, j is a cyclic pair, $\cos\theta = \hat{q}_i \cdot \hat{q}_j$, and

$$a_{ij} = \frac{W_i^2 - q_i^2 + m_j^2 - m_k^2 + 2\sqrt{(m_j^2 + q_j^2)(W_i^2 - q_i^2)}}{2\sqrt{W_i^2 - q_i^2} \left(W_i + \sqrt{W_i^2 - q_i^2} \right)}, \quad (40)$$

$$a_{ji} = \frac{W_j^2 - q_j^2 + m_i^2 - m_k^2 + 2\sqrt{(m_i^2 + q_i^2)(W_j^2 - q_j^2)}}{2\sqrt{W_j^2 - q_j^2} \left(W_j + \sqrt{W_j^2 - q_j^2} \right)}, \quad (41)$$

with

$$W_i = \sqrt{m_j^2 + q_j^2} + \sqrt{m_k^2 + (\vec{q}_i + \vec{q}_j)^2}, \quad (42)$$

$$W_j = \sqrt{m_i^2 + q_i^2} + \sqrt{m_k^2 + (\vec{q}_i + \vec{q}_j)^2}. \quad (43)$$

Eqs. (39)-(43) correspond to relativistic kinematics for three particles on the mass shell.

In order to find the eigenvalues of the integral equations (30)-(32), integrals were replaced by sums applying numerical integration quadrature. In this way the equations become a

set of homogeneous linear equations which have solutions only if the determinant of the matrix of its coefficients (the Fredholm determinant) vanishes at certain (complex) energies. We used the standard procedure described in Ref. [20], i.e., we make the contour rotation $q_i \rightarrow q_i \exp(-i\phi)$ which opens some portions of the second Riemann sheet for the variable W_0 . This allows one to look for poles of Eqs. (30)-(32) by taking $W_0 = M - i\Gamma/2$, and calculating the Fredholm determinant to look for its zeros.

IV. RESULTS AND DISCUSSION

Before reporting the results of a full three-body Faddeev calculation for the $\bar{K}N\pi\text{--}\pi Y\pi$ coupled channels, we discuss some relevant partial calculations.

- Limiting the Faddeev equations to the lower $\pi Y\pi$ three-body channel, for various combinations of the input two-body interactions, resonance poles about 200 MeV above the $\bar{K}N\pi$ threshold are obtained. The p -wave πY and $\pi\pi$ interactions used were those described in Sec. II, whereas separable interactions corresponding to the scattering length and effective radius combinations listed by Ikeda *et al.* [21] for the $I_3 = 0$ $\pi\Sigma$ interaction were constructed to simulate the s -wave πY interaction. This interaction which is used in meson-baryon chiral models is too weak to help bind the $\pi Y\pi$ system, much the same as it is too weak in a two-body calculation to generate on its own a resonance similar to $\Lambda(1405)$, without coupling in the $I_3 = 0$ $\bar{K}N$ upper channel interaction.
- Limiting the Faddeev equations to the upper $\bar{K}N\pi$ three-body channel, for various combinations of the input two-body interactions, resonance poles about 100 MeV above the $\bar{K}N\pi$ threshold are obtained. The p -wave πN and $\pi\bar{K}$ interactions used were those described in Sec. II. In these calculations, the $I_3 = 0$ $\bar{K}N$ s -wave interaction used was sufficiently strong to bind on its own in the range of $M_{\bar{K}N} \sim 1420\text{--}1430$ MeV.
- Using a complex $I_3 = 0$ $\bar{K}N$ s -wave interaction in the $\bar{K}N\pi$ three-body Faddeev calculations, to simulate implicitly coupling to the lower $\pi Y\pi$ channel, the $\bar{K}N\pi$ resonance energy decreased as low as to about 50 MeV above the $\bar{K}N\pi$ threshold. Here, the $I_3 = 0$ $\bar{K}N$ scattering length was fixed at $a_3 = -1.70 + i0.68$ fm [16] and

the real part of the fitted separable scattering amplitude changed sign at around 1405 MeV, with a quasibound pole in the range $M_{\bar{K}N} \sim 1415\text{--}1425$ MeV.

TABLE IV: Energy eigenvalue of the $\bar{K}N\pi$ system for the several models of the $I = 1$ πY p -wave interaction given in Table II and the models of the $\bar{K}N$, $\bar{K}\pi$, πN , and $\pi\pi$ interactions given in Tables I and III.

$A(\text{fm}^2)$	$W_0 - m_{\bar{K}} - m_N - m_{\pi}$ (MeV)
0.00	$-111.0 - i0.1$
0.05	$-67.5 - i1.4$
0.10	$-42.1 - i6.4$
0.15	$-26.1 - i13.0$
0.20	$-15.4 - i20.6$
0.25	$-7.6 - i24.6$
0.30	$-1.2 - i29.5$
0.35	$+3.6 - i32.4$
0.40	$+7.8 - i34.3$
0.45	$+10.9 - i35.2$
0.50	$+12.8 - i37.4$

Finally, the full $\bar{K}N\pi\text{--}\pi Y\pi$ coupled channel Faddeev equations were solved. Table IV lists the energy eigenvalues with respect to the $\bar{K}N\pi$ threshold obtained for the models of the $\bar{K}N$, $\bar{K}\pi$, πN , and $\pi\pi$ interactions specified in Tables I and III, and models of the $I = 1$ πY p -wave interaction given in Table II. Singling out πY form factors in the range $A = 0.25$ to $A = 0.45$ fm² from Table II, with values of r_0 up to 0.15 fm larger than the πN value $r_0 = 1.36$ fm from Table III, as discussed in subsection II E, a $I(J^P) = 1(\frac{3}{2}^-)$ $\bar{K}N\pi$ resonance or quasibound state is predicted near the $\bar{K}N\pi$ threshold, with mass $M \approx (1570 \pm 10)$ MeV and partial decay width $\Gamma_{\downarrow} \approx (60 \pm 10)$ MeV. This partial width excludes contributions from channels disregarded in the present $\bar{K}N\pi\text{--}\pi Y\pi$ three-body model. The total width $\Gamma = \Gamma_{\downarrow} + \Gamma_{\uparrow}$ includes also a partial width Γ_{\uparrow} induced by meson absorption modes into two-body $\bar{K}N$ and πY final states which were disregarded in this exploratory calculation and could amount to several tens of MeV.

V. SUMMARY

In this work we have derived three-body Faddeev equations for the $\bar{K}N\pi$ - $\pi Y\pi$ coupled channels, with isobar model separable p -wave interactions for the two-body πN ($\Delta(1232)$), $\pi\bar{K}$ ($K^*(892)$), πY ($\Sigma(1385)$) and $\pi\pi$ ($\rho(770)$) subsystems, and separable s -wave coupled channel interactions for the two-body $\bar{K}N$ - πY subsystem dominated by the $\Lambda(1405)$ resonance. We solved these Faddeev equations, with two-body separable interactions fitted to available data, searching for a $I(J^P) = 1(\frac{3}{2}^-)$ $\bar{K}N\pi$ quasibound state. All the resonating two-body subsystems used for input in the coupled channels Faddeev calculation were found indispensable to obtain a quasibound solution near the $\bar{K}N\pi$ threshold. The uncertainty of this calculation is determined by the lack of a reliable p -wave phase shift parametrization for the $\Sigma(1385) \rightarrow \pi Y$ decay spectrum. Requiring a ‘size’ of the πY form factor similar to that for πN , a $\bar{K}N\pi$ resonance or quasibound state exists with mass $M \approx (1570 \pm 10)$ MeV and decay width which is bounded from below by $\Gamma_{\downarrow} \approx (60 \pm 10)$ MeV. With respect to two-body $\bar{K}N$ and πY final states, which are outside the scope of the present three-body model, this $\bar{K}N\pi$ state defines a D_{13} Σ resonance near the $\bar{K}N\pi$ threshold. The PDG listing [4] leaves room for a resonance in this mass range, with the two-star ‘bumps’ $\Sigma(1560)$ and the one-star $I(J^P) = 1(\frac{3}{2}^-)$ $\Sigma(1580)$ as possible candidates. In particular, the known two-body $\bar{K}N$ and πY decay branching ratios are abnormally small for $\Sigma(1580)$, indicating that their partial width Γ_{\uparrow} is smaller than the partial width Γ_{\downarrow} for two-meson decay modes $\bar{K}N\pi \rightarrow \pi Y\pi$ of the present model.

Acknowledgments

This work was supported in part by the EU initiative FP7, HadronPhysics2, under Project No. 227431, and in part by COFAA-IPN (México).

-
- [1] A. Gal, in *From Nuclei to Stars, Festschrift in Honor of Gerald E. Brown*, Ed. Sabine Lee (World Scientific, 2011) pp. 157-170 [arXiv:1011.6322 (nucl-th)].
 - [2] A. Gal, and H. Garcilazo, Phys. Rev. D **78**, 014013 (2008).
 - [3] H. Garcilazo, and A. Gal, Phys. Rev. C **81**, 055205 (2010).

- [4] <http://pdglive.lbl.gov>
- [5] K.P. Khemchandani, A. Martinez Torres, and E. Oset, Eur. Phys. J. A **37**, 233 (2008).
- [6] D. Jido, and Y. Kanada-En'yo, Phys. Rev. C **78**, 035203 (2008).
- [7] A. Martinez Torres, K.P. Khemchandani, and E. Oset, Phys. Rev. C **79**, 065207 (2009).
- [8] A. Martinez Torres, and D. Jido, Phys. Rev. C **82**, 038202 (2010).
- [9] A. Martinez Torres, K.P. Khemchandani, and E. Oset, Phys. Rev. C **77** 042203(R) (2008).
- [10] Y. Kanada-En'yo, and D. Jido, Phys. Rev. C **78**, 025212 (2008).
- [11] K.P. Khemchandani, A. Martinez Torres, and E. Oset, Phys. Lett. B **675**, 407 (2009).
- [12] T. Hyodo, and D. Jido, Prog. Part. Nucl. Phys. **67**, 55 (2012).
- [13] Y. Ikeda, H. Kamano, and T. Sato, Prog. Theor. Phys. **124**, 533 (2010).
- [14] J.E. Conboy *et al.*, J. Phys. G **12**, 1143 (1986), and references therein.
- [15] J.K. Kim, Phys. Rev. Lett. **19**, 1074 (1967).
- [16] A.D. Martin, Nucl. Phys. B **179**, 33 (1981).
- [17] R.A. Arndt, W.J. Briscoe, I.I. Strakovsky, and R.L. Workman, Phys. Rev. C **74**, 045205 (2006).
- [18] D.R. Boito, E. Escribano, and M. Jamin, JHEP **1009**, 031 (2010).
- [19] S.D. Protopopescu *et al.*, Phys. Rev. D **7**, 1279 (1973).
- [20] B.C. Pearce, and I.R. Afnan, Phys. Rev. C **30**, 2022 (1984).
- [21] Y. Ikeda, T. Hyodo, D. Jido, H. Kamano, T. Sato, and K. Yazaki, Prog. Theor. Phys. **125**, 1205 (2011).